JACS
JOURNAL OF THE AMERICAN CHEMICAL SOCIETY
Article
pubs.acs.org/JACS

A Macrocyclic Chelator with Unprecedented Th^{4+} Affinity

Tiffany A. Pham,[†,‡] Jide Xu,[†,‡] and Kenneth N. Raymond*[,†,‡]

[†]Department of Chemistry, University of California, Berkeley, Berkeley, California 94720-1460, United States
[‡]Chemical Sciences Division, Lawrence Berkeley National Laboratory, Berkeley, California 94720-1460, United States

Supporting Information

ABSTRACT: A novel macrocyclic octadentate ligand incorporating terephthalamide binding units has been synthesized and evaluated for the chelation of Th^{4+}. The thorium complex was structurally characterized by X-ray diffraction and in solution with kinetic studies and spectrophotometric titrations. Dye displacement kinetic studies show that the ligand is a much more rapid chelator of Th^{4+} than prevailing ligands (1,4,7,10-tetraazacyclododecane-1,4,7,10-tetraacetic acid and diethylenetriaminepentaacetic acid). Furthermore, the resulting complex was found to have a remarkably high thermodynamic stability, with a formation constant of 10^{54}. These data support potential radiotherapeutic applications.

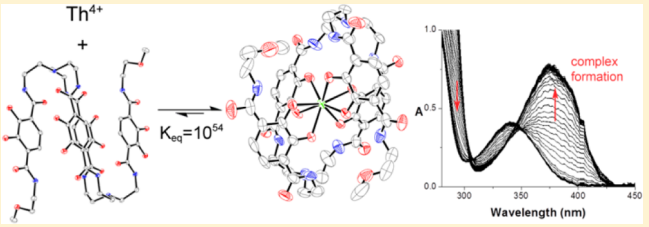

INTRODUCTION

α-Particle emitters have been studied for applications in radiotherapy for over 50 years.[1] The shorter range and higher energy of α-particles relative to β-particles results in greater cytotoxicity.[2] However, clinical investigations of α-therapeutics are fairly recent. Nuclear therapy was previously limited to β-emitters and external radiation. To date, the only FDA-approved α-emitter is $^{223}RaCl_2$, a calcium mimic effective in the treatment of bone metastases.[3] Coupling the short-range of α-particles with the precise targeting of a biomolecule, such as an antibody, could offer radiotherapeutics with both the advantages of versatility and specificity. Much of the current research in α-therapy is directed toward using a variety of α-emitters, e.g., ^{225}Ac, ^{211}At, ^{227}Th, ^{213}Bi,[4] in conjunction with a ligand covalently attached to a biomolecule. This approach has created a demand for suitable chelators, which must rapidly and irreversibly form thermodynamically stable complexes with the α-emitting radioisotope under physiological conditions. Published approaches have been limited to aminocarboxylic acids such as diethylenetriaminepentaacetic acid (DTPA) and 1,4,7,10-tetraazacyclododecane-1,4,7,10-tetraacetic acid (DOTA) and their derivatives. While these chelators have been available for several decades, their effectiveness is in several respects quite limited.

Algeta ASA, the producer of the commercialized $^{223}RaCl_2$, has pointed out the potential of ^{227}Th, a β-decay product of ^{227}Ac.[5] This α-emitter decays to ^{223}Ra with an 18.7 d half-life, a convenient time scale for manufacturing and shipping. However, unlike radium, the chemistry of thorium requires its sequestration in a stable complex. If then attached to a targeting agent such as a monoclonal antibody, various ^{227}Th therapeutic agents could be envisioned. However, current available chelators do not simultaneously have high thermodynamic stability and fast association. In general, macrocycles such as DOTA have both slow off and on rates, while acyclic ligands like DTPA display faster formation kinetics but form complexes of lower stability. For example, DOTA has a greater stability with lanthanides than DTPA by about 2 orders of magnitude, but the latter displays faster kinetics by 4 orders of magnitude.[6]

Our siderophore-inspired ligands have been used to complex actinides for applications in nuclear waste remediation and in vivo decorporation.[7] The terephthalamide (TAM) binding group has a very high binding affinity for Th^{4+},[7c] and its two amide groups enable its incorporation in a novel ligand topology intended to address the requirements for a good radiotherapeutic chelate. The ligand **L** (Figure 1) was designed

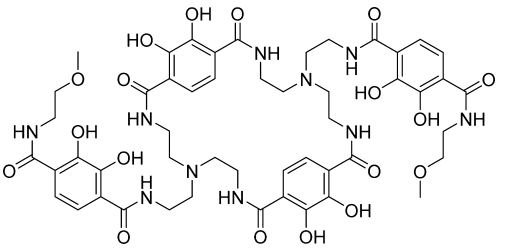

Figure 1. Octadentate terephthalamide ligand (**L**) with a topology incorporating a macrocycle with pendant binding units.

to combine the favorable thermodynamics of macrocycles with the favorable kinetics of linear ligands. It features four binding units (at least eight atoms are required to fill the coordination sphere of Th^{4+}): two TAMs in a macrocycle and two TAMs on pendant arms, connected by tris(2-aminoethyl)amine (tren) backbones. The pendant TAMs provide opportunities for

Received: April 10, 2014

   dx.doi.org/10.1021/ja503456r | J. Am. Chem. Soc. XXXX, XXX, XXX−XXX

Scheme 1. Synthesis of L[a]

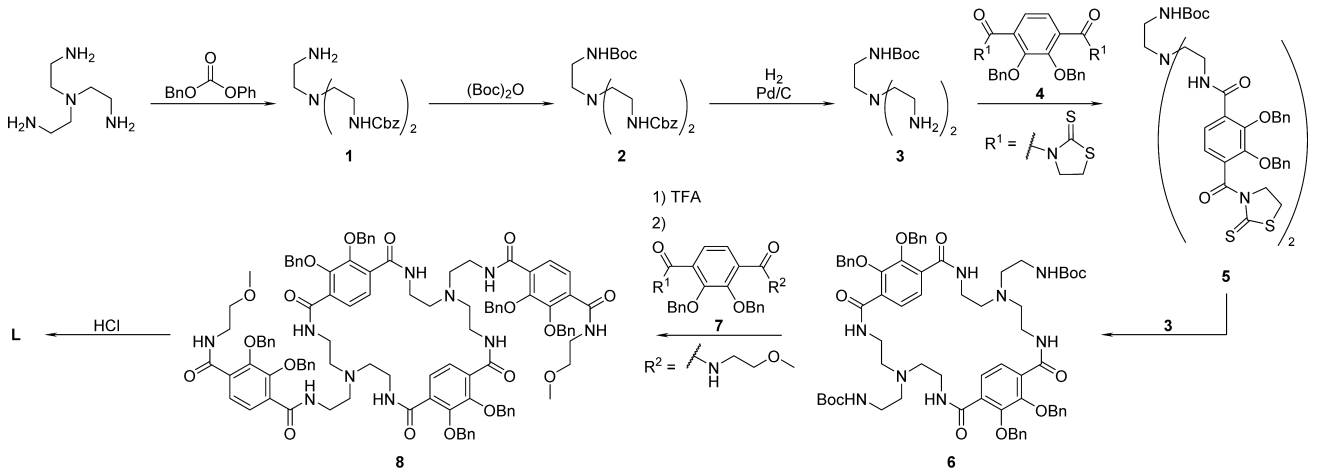

[a]Complete experimental procedures and abbreviations are detailed in the Experimental Section.

further functionalization, e.g., for linking to a targeting moiety. In **L** they were functionalized with methoxyethyl groups to increase the water solubility of the untargeted ligand. The suitability of **L** as a Th^{4+} chelator for radiotherapeutic applications was evaluated with thermodynamic, kinetic, and single-crystal X-ray diffraction (XRD) studies.

RESULTS AND DISCUSSION

Synthesis of L. The synthesis of **L** (Scheme 1) was adapted from known preparations of analogous ligands.[7a] For ease of purification the singly protected tren **3** was accessed in three steps; the one-step synthesis[8] gave a mixture of singly and doubly protected amines that could not be separated. Two of the tren amines were protected with benzyloxycarbonyl (Cbz) groups (yielding **1**), which were removed by hydrogenolysis following protection of the remaining amine with a *tert*-butoxycarbonyl (Boc) group (forming **2**). Another key intermediate was the macrocycle, which was formed with two high-dilution reactions to prevent undesired polymeric by-products.[9] Compound **5** was formed by the slow addition of mono-Boc tren (**3**) into a large excess of the TAM derivative **4**, while **6** was formed by the slow addition of the reactants, in equimolar amounts, into a large volume of solvent. Deprotection of the Boc groups in the presence of the benzyl protecting groups proved slightly problematic, since the benzyl groups were also susceptible to cleavage. This problem was circumvented by using milder reaction conditions (30% trifluoroacetic acid in CH_2Cl_2, added dropwise at 0 °C, followed by reaction at room temperature monitored by TLC) and prompt quenching with triethylamine as soon as the deprotection reached completion. Attempts to isolate the primary amine of **6** were unsuccessful, and coupling to the pendant TAMs was performed immediately following quenching of the Boc deprotection.

Mass spectral and elemental characterization of **L** confirmed its identity, but the ^{1}H NMR in DMSO showed extensive hydrogen bonding that broke the symmetry, affording a complicated spectrum. Treatment of **L** with NaOD in D_2O restored the expected symmetry and yielded well-resolved ^{1}H NMR signals.

Structural Characterization of L and ThL. Single crystals suitable for XRD were grown by the vapor diffusion of acetonitrile into an aqueous solution of the free ligand. The thorium complex was in turn crystallized from a methanol and dimethylformamide solution, into which diethyl ether and tetrahydrofuran were diffused. Naturally occurring ^{232}Th, which has a half-life of 1.4×10^{10} years, was used for ease of handling. XRD experiments gave the structures of **L** and its thorium complex (Figure 2, Table 1).

In principle, the macrocyclic TAMs of the ligand could chelate a metal ion in two possible configurations, either equatorially, with the pendant units on opposite sides of the metal–macrocycle plane (pseudo-C_{2h} symmetry) or in a configuration of lower symmetry (pseudo-C_2 symmetry), where the pendant arms are adjacent to one another (Figure 3). As the protonated ligand, **L** crystallizes with inversion symmetry (as in the pseudo-C_{2h}), but was observed to adopt the C_2-symmetric conformation around the metal center when bound to Th^{4+}. DFT-level calculations [B3LYP/6-31G, SDD-(f)][10] of the complex in these two possible conformations suggest that the observed mode is the more thermodynamically stable one. The calculated C_2-symmetric structure with adjacent pendant units is 22 kcal/mol lower in energy than the corresponding C_{2v}-symmetric structure, a stabilization that can be attributed to the macrocyclic strain induced by the large diameter of Th^{4+}. Increasing the ring size with tris(2-aminopropyl)amine (trpn) instead of tren in the ligand backbones reduces this calculated energy difference to 13 kcal/mol. The inner coordination environment of the crystallized complex was analyzed with a quantitative shape measure (SM),[11] which compares the dihedral angles of adjacent faces in the crystal structure's coordination polyhedron to those of idealized polyhedra most common in eight-coordinate complexes: the bicapped trigonal prism (C_{2v}), trigonal dodecahedron (D_{2d}), and square antiprism (D_{4d}). The coordination of Th**L** about the metal center is intermediate between the ideal C_{2v} and D_{2d} geometries [SM = 5.3 (C_{2v}), 7.7 (D_{2d}), and 11.1 (D_{4d})]. Despite considerable distortion, the TAM binding units can be viewed as spanning the *m* edges of a trigonal dodecahedron with angles of 1.0°, 2.7°, 14.7°, and 19.5° from vertical.[12] The macrocyclic binding units have the largest deviation angles, providing further evidence for the overall chelation mode of the ligand being attributable to ring strain.

Kinetics. Radiotherapeutics are inherently time-sensitive, as the radioisotope must be fully sequestered by the chelate as fast

dx.doi.org/10.1021/ja503456r | J. Am. Chem. Soc. XXXX, XXX, XXX–XXX

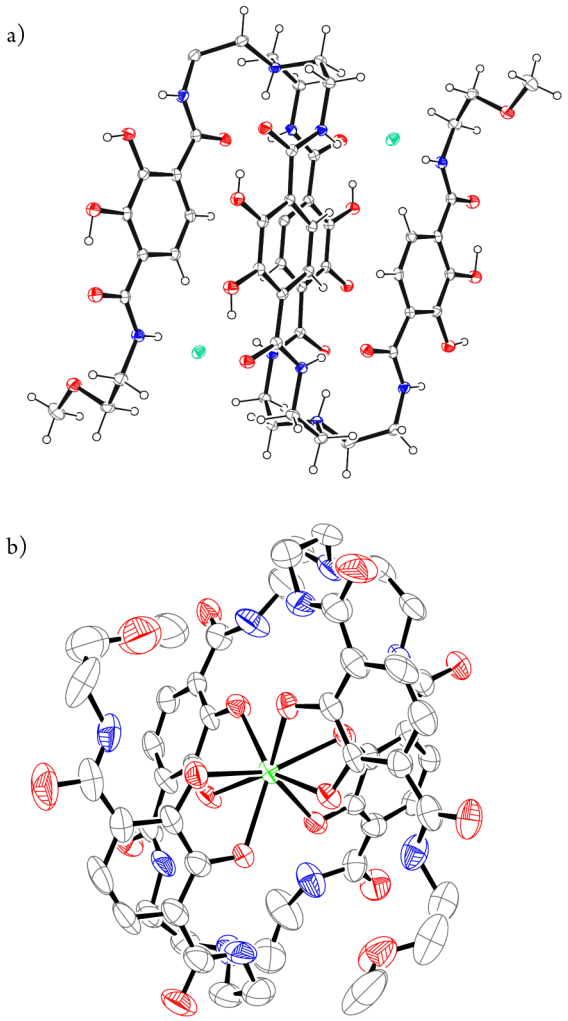

Figure 2. ORTEP diagrams of (a) the protonated ligand $\mathbf{L}H_8{\cdot}2HCl$ and (b) the $[Th\mathbf{L}]^{4-}$ complex. Potassium ions, solvent molecules, and hydrogens in part b are omitted for clarity. Ellipsoids are shown at 50% probability (gray, C; red, O; blue, N; green, Cl; lime-green, Th).

as possible to minimize decay prior to administration to the patient. In addition to entropic effects, the high thermodynamic stability of macrocycles with metal ions is attributed to the preorganization of the donor atoms and multiple juxtapositional fixedness, which describes the greater difficulty with which the donor atoms dissociate due to the lack of end groups.[13] However, the rigidity of the ligand causing this stability can also hinder its kinetics of complexation. For example, the polyaminocarboxylic acid macrocycles DOTA and HEHA have slow formation rates with Ln(III) ions.[6c,14] Despite this shortcoming, DOTA is among the most commonly studied macrocycles in radioactive medical applications,[15] but an ideal bifunctional chelator would form the final complex quickly under mild conditions, to avoid damaging the targeting biomolecule.

Study of the kinetics of association posed several problems due to the spectroscopic silence of Th^{4+}, as well as its propensity to hydrolyze. By UV−vis spectroscopy, complexation could only be monitored by changes in **L**, as there are no distinct charge-transfer bands with Th^{4+}. However, at physiological pH and in excess of ligand, the spectral difference between the ligand and the Th**L** complex is small (Figure 4a), rendering accurate monitoring of the reaction difficult. Furthermore, above pH 3.1, more than 50% of the Th in solution is hydrolyzed ($[ThOH]^{3-}$, $[Th(OH)_2]^{2-}$, $[Th_4(OH)_{12}]^{4+}$, etc.[16]), and increasingly more so at higher pH values. In order to simplify the mechanism of complexation by **L**, the metal was maintained as mainly free Th^{4+} in acidic solution (pH 1.4, in 79 mM HNO_3) until mixing with **L**, which was buffered such that mixing with the Th solution resulted in a reaction mixture at pH 7.4. The reaction studied was then

$$Th^{4+} + \mathbf{L}H_n^{-8+n} \rightarrow [Th\mathbf{L}]^{4-} + nH^+ \quad (1)$$

At this pH, most of the ligand is present as $\mathbf{L}H_4^{4-}$ and $\mathbf{L}H_5^{3-}$ (the species present in greater than 1% are $\mathbf{L}H_4^{4-}$, $\mathbf{L}H_5^{3-}$, and $\mathbf{L}H_6^{2-}$, at 39.1, 57.8, and 2.6%, respectively). These measurements were conducted using a stopped-flow apparatus, allowing UV spectra to be taken immediately following the fast mixing of the metal and ligand solutions. With various excess ligand concentrations, the complexation was performed under pseudo-first order kinetic conditions, from which a second-order rate constant could be calculated. The observed first-order rate constants [determined using the regression modeling program Specfit[17] to fit the changes in absorbance (Figure 4b) at a range of wavelengths] were linearly dependent on the ligand concentration, suggesting a second-order reaction with a rate constant of $k_2 = 1.8(1) \times 10^4\ M^{-1}\ s^{-1}$ (the slope of the linear regression in Figure 4c). The half-life of the complexation of 1 μM Th and 1 μM **L** is then 57 s, a more than adequately short time period for radiotherapeutic applications of **L**. The direct comparison of the k_2 value with those of other ligands is not possible given the lack of published work on the rate of complexation of Th^{4+} by relevant ligands.

Of particular interest is the improved complexation kinetics of **L** as compared to DTPA and DOTA, and the stopped-flow kinetic experiment performed above is not applicable because the ligands do not absorb in the UV−vis region. The relative rate of complexation of Th^{4+} was instead studied indirectly, using the dye Arsenazo III (D), with which it forms a colored complex. The addition of ligand (**L**, DTPA, or DOTA) displaced the dye, and the formation of a thorium−ligand complex could be monitored by disappearance of the thorium−dye complex (Figure 5b). The reaction effectively became the ligand exchange described by the following general equation:

$$ThD + \mathbf{L} \rightarrow Th\mathbf{L} + D \quad (2)$$

The stoichiometry of the thorium−dye complex, measured with a Job plot (Figure 5a), was found to be between 1:1 and 1:2 Th:dye, varying with the purity of the dye used. Previous work[18] supports the existence of the 1:2 species, and since the exact stoichiometry of the complex was not crucial for this indirect kinetic study, an excess of dye was used to ensure that all of the thorium was complexed. The Th−dye complex was formed at acidic pH, to avoid the presence of Th hydroxide species, and buffered to pH 7.4 prior to mixing with the ligand. The aim was to extrapolate a second-order rate constant by performing this displacement reaction under pseudo-first-order conditions at different concentrations of excess ligand. However, a rate dependence on the **L** concentration was not observed under conditions above 10 equiv of **L** relative to Th^{4+}. A second-order rate constant was then calculated only for the reactions with this ligand concentration, which was sufficient for qualitative comparisons (Table 2); **L** was found to complex Th with an observed rate constant of 147 $M^{-1}\ s^{-1}$, a value 2 orders of magnitude greater than those of DTPA (0.61 $M^{-1}\ s^{-1}$). No dye displacement was observed with DOTA over 2

dx.doi.org/10.1021/ja503456r | J. Am. Chem. Soc. XXXX, XXX, XXX−XXX

Table 1. Crystallographic Data and Structure Refinement for $LH_8{\cdot}2HCl{\cdot}4H_2O$ and $ThLK_4{\cdot}(DMF)_2{\cdot}(MeOH)_2{\cdot}THF$

empirical formula	$C_{50}H_{72}Cl_2N_{10}O_{22}$	$C_{62}H_{84}K_4N_{12}O_{23}Th$
M_r	1236.08 g/mol	1753.85 g/mol
temp	100(2) K	130(2) K
wavelength	1.54178 Å	0.71073 Å
crystal system	monoclinic	triclinic
space group	$P2_1/n$	$P\bar{1}$
unit cell dimensions	a = 11.0189(6) Å, α = 90°	a = 11.347(2) Å, α = 79.129(2)°
	b = 8.3701(4) Å, β = 94.475(2)°	b = 16.549(2) Å, β = 87.126(2)°
	c = 29.9278(15) Å, γ = 90°	c = 20.044(3)Å, γ = 79.929(2)°
volume	2751.8(2) Å^3	3638.8(8) Å^3
Z	2	2
ρ_{calcd}	1.492 g/cm^3	1.551 g/cm^3
μ_{calcd}	1.849 mm^{-1}	2.357 mm^{-1}
F(000)	1304	1719
crystal size	0.10 × 0.50 × 0.10 mm^3	0.21 × 0.09 × 0.06 mm^3
2θ range for data collection	2.96°−68.34°	1.03°−50.74°
index ranges	$-13 \le h \le 11$, $-10 \le k \le 10$, $-36 \le l \le 34$	$-13 \le h \le 13$, $-19 \le k \le 16$, $-24 \le l \le 24$
reflections collected	48 118	45 683
independent reflections	5013 [R(int) = 0.0294]	13322 [R(int) = 0. 0928]
completeness to θ = 25.00°	99.6%	99.9%
absorption correction	semiempirical from equivalents	semiempirical from equivalents
max and min transmission	0.8367 and 0.2593	0.8715 and 0.6374
refinement method	full-matrix least-squares on F^2	full-matrix least-squares on F^2
data/restraints/parameters	5013/0/432	13322/102/954
goodness-of-fit on F^2	1.037	1.038
final R indices [$I > 2\sigma(I)$]	R_1 = 0.0355, wR_2 = 0.0919	R_1 = 0.0709, wR_2 = 0.1711
R indices (all data)	R_1 = 0.0432, wR_2 = 0.0965	R_1 = 0.1147, wR_2 = 0.1973
largest diff peak and hole	0.673 and −0.268 e Å^{-3}	1.568 and −1.564 e Å^{-3}

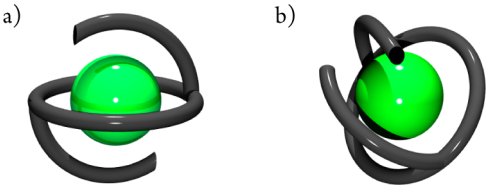

Figure 3. Diagrams illustrating possible chelation modes of Th^{4+} by **L**. (a) Pseudo-C_{2h} symmetric structure, where the pendant TAMs lie on opposite sides of the equatorially bound macrocyclic TAMs. (b) Pseudo-C_2 symmetric structure as observed in the crystal structure, where the pendant TAMs are on the same side of the macrocycle.

months at room temperature; it only proceeded within a practicable time upon heating (100 °C). Despite the uncertain mechanism in these dye displacement experiments—the rate-limiting step is most likely dye dissociation rather than ligand association in the presence of a fast ligand—**L** is clearly a much faster thorium chelator than the macrocyclic DOTA and the linear DTPA. These faster kinetics can be attributed to the greater affinity of TAM relative to the O and N donors in DTPA and DOTA but likely also to the partially macrocyclic topology of **L**. Much like a linear ligand, its pendant arms afford greater flexibility that enable faster association to the metal ion.

Thermodynamics. The thermodynamic stability of the Th**L** complex was also evaluated. This property is of high importance, as the release of the metal ion would be catastrophic. Thorium forms hydroxides and complexes with many proteins, amino acids, and other biological molecules, which can aggregate in internal organs, such as the liver and spleen.[19] Due to the high number of pK_a values and moderate water solubility, UV−vis spectrophotometric titrations were performed to determine the protonation and Th formation constants of **L**. Although the pK_a values of the hydroxyl groups of a bidentate TAM unit are 6.0 and 11.0,[20] those in **L** range from 3.95 to 12.79 (Table 3). Statistical factors alone do not account for this wide range, indicating further intramolecular interactions within the various deprotonated states. As is apparent in the representative titration shown in Figure 6, a large pH range was required to attain all the protonation states of **L**, and the UV−vis spectra of the individual species (Figure 9) display significant overlap.

Measurement of the Th^{4+} stability constant required the use of a competing ligand in excess; otherwise, Th**L** would already be formed at the start of the titration at pH 2. In the presence of DTPA, the Th−DTPA complex instead forms at this low pH, and at approximately pH 4, the $[ThLH]^{3-}$ complex begins to form, which can be monitored spectrophotometrically. The largest change in absorbance occurs at pH 5−6, when the $[ThLH]^{3-}$ becomes deprotonated to form $[ThL]^{4-}$ (Figure 7).

The log β_{110} (where β_{mlh} is the cumulative stability constant for the equilibrium $m\mathrm{M} + l\mathrm{L} + h\mathrm{H} \rightleftharpoons \mathrm{M}_m\mathrm{L}_l\mathrm{H}_h$) was found to be 53.7(5), 24 orders of magnitude greater than that of DTPA (28.78,[21] Table 4). Its greater log β_{110} value relative to the log β_{140} = 45.54 for ethyl-TAM[7b] suggests that the higher denticity and/or macrocyclic topology confers substantial thermodynamic stability to the Th**L** complex. A measure of the complex stability is also provided by the pTh value,[22] or the −log of the free thorium concentration at a specific pH and $[Th]_{tot}$ = 1 μM and $[L]_{tot}$ = 10 μM (the speciation diagram in Figure 8 shows the dominant species in the pH 1−13 range). This value accounts for the effect of protonation on metal−ligand equilibria, providing a direct comparison of the complexing abilities of various ligands, which have different protonation constants under physiologically relevant conditions. While

dx.doi.org/10.1021/ja503456r | J. Am. Chem. Soc. XXXX, XXX, XXX−XXX

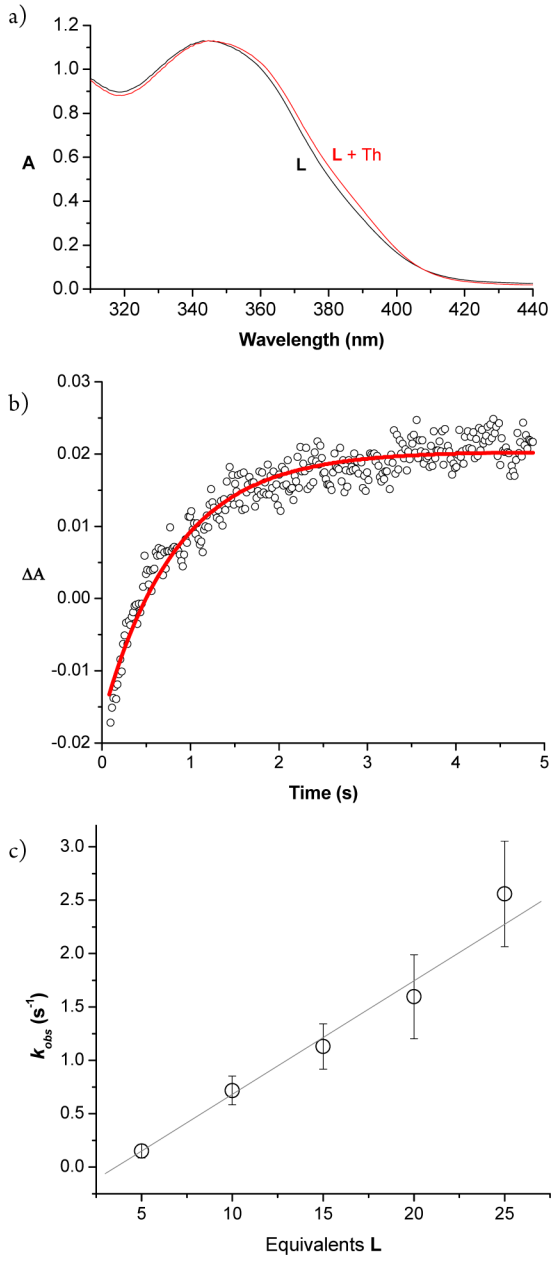

Figure 4. Direct kinetics. Stopped-flow experimental conditions: pH 7.4 upon 1:1 mixing of Th^{4+} (pH 1.4, 79 mM HNO_3) and **L** (pH 8.2, 200 mM HEPES, 10% DMSO), 25 °C. (a) UV−vis spectra of **L** (before mixing with Th) and Th**L** (10 s after mixing, 5 μM Th, 10 equiv of **L**). (b) *A* vs *t* plot of complexation of Th by **L** upon mixing at t = 0 (5 μM Th, 15 equiv of **L**) at 380 nm (black circles represent experimental values; the red line is the first-order fit). (c) Observed first-order rate constants (error bars are standard deviations) calculated at varying concentrations of **L** relative to thorium. The second-order rate constant was extrapolated from the slope of the linear regression.

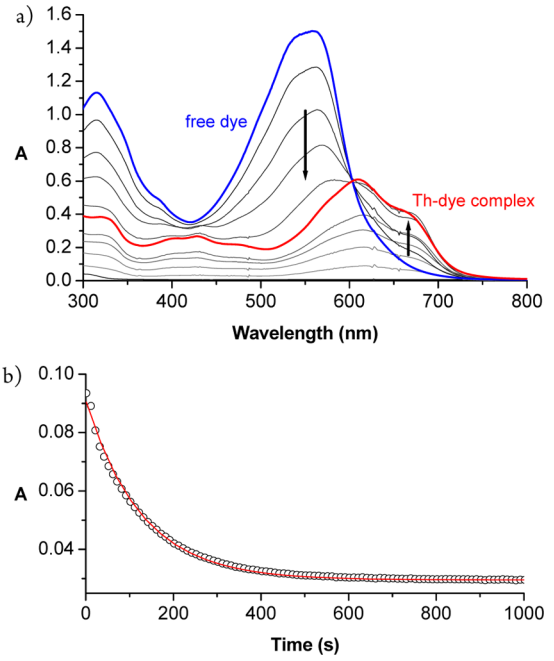

Figure 5. Indirect kinetics. (a) UV−vis spectra of free Arsenazo III dye (blue, 50 μM) and of Th−dye complex (red, 25 μM dye and 25 μM Th) at pH 7.4 (100 mM HEPES, 0.1 M KCl). Spectra in black are of Th and dye at intermediate stoichiometries (arrows denote spectral changes with increasing concentrations of Th). (b) *A* vs *t* plot at 669 nm, showing the displacement of dye from the Th−dye complex upon addition of **L** at t = 0 (5 μM Th−dye, 50 μM **L**, pH 7.4, 100 mM HEPES, 0.1 M KCl, 25 °C). Black circles are data points; the red line is the first-order exponential decay fit (R^2 = 0.9974).

Table 2. Indirect Kinetic Data[a] for L, DTPA, and DOTA

ligand	k_{obs} (M^{-1} s^{-1})
L	147
DTPA	0.61
DOTA[b]	0.93

[a]Reaction conditions: 5 μM Th−Arsenazo III complex, 50 μM ligand, pH 7.4 (100 mM HEPES, 100 mM KCl), 25 °C. Rates calculated from the decrease in absorbance at 669 nm (Th−Arsenazo III complex). [b]100 °C.

Table 3. pK_a Values of L

pK_{a1}	12.79(2)
pK_{a2}	11.9(4)
pK_{a3}	11.1(2)
pK_{a4}	9.3(4)
pK_{a5}	7.57(9)
pK_{a6}	6.1(6)
pK_{a7}	5.73(6)
pK_{a8}	3.95(4)
pK_{a9}	3.30(7)
pK_{a10}	1.9(2)

DTPA has a higher pTh at low pH, due to its greater acidity, **L** has a remarkably higher pTh at neutral and higher pH, implying negligible Th dissociation from **L** in vivo.

CONCLUSION

Solution thermodynamic studies have shown an unprecedented Th^{4+} binding affinity for the ligand **L**, and while kinetic studies did not provide a similarly quantitative measure, the indirect dye kinetics enabled the direct comparison of the metal complexation rates of **L** with other ligands, in particular the prevailing chelators DTPA and DOTA. In the metal complex the terephthalamide binding units are arranged in a novel topology that may explain the fast complexation and high stability.

dx.doi.org/10.1021/ja503456r | J. Am. Chem. Soc. XXXX, XXX, XXX−XXX

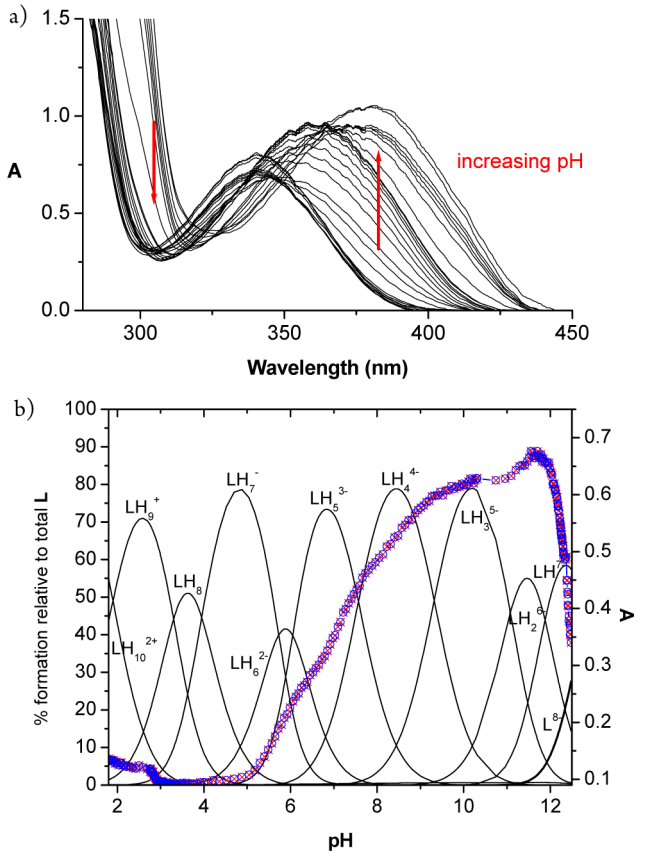

Figure 6. Spectrophotometric titration of **L**. Starting conditions: 70 μM **L**, 0.1 M KCl, and 1 mM each of MES, HEPES, and CHES (25 °C). (a) *A* vs wavelength plot at varying pH (data abridged for clarity; spectra normalized for dilution). (b) *A* vs pH at 380 nm (experimental data points are blue circles, red crosses are calculated absorbances) overlaid onto speciation.

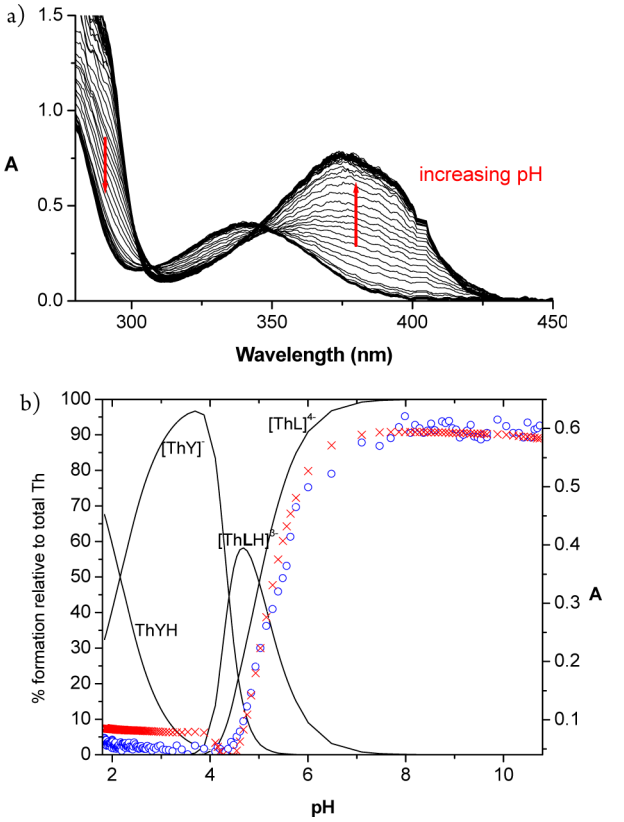

Figure 7. Spectrophotometric competition titration of Th**L**. Starting conditions: 50 μM Th, 50 μM **L**, 1 mM DTPA, and 0.1 M KCl (25 °C). (a) *A* vs wavelength plot at varying pH (data abridged for clarity; spectra normalized for dilution). (b) *A* vs pH at 380 nm (experimental data points are blue circles, red crosses are calculated absorbances) overlaid onto speciation.

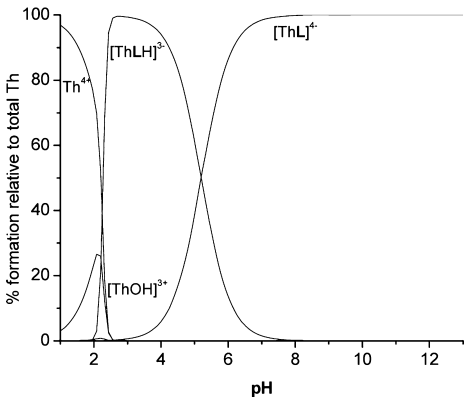

Figure 8. Speciation diagram at [**L**] = 10 μM and [Th] = 1 μM.

EXPERIMENTAL SECTION

Synthesis. All chemicals were used as supplied without further purification, unless otherwise noted. Characterization data were obtained at facilities at the University of California, Berkeley, except for the elemental analysis of **L**, which was also performed by Columbia Analytical Services (Tucson, AZ). NMR spectra were obtained at room temperature on Bruker AV-500 or AV-600 spectrometers. Chemical shifts are reported in parts per million (ppm) relative to solvent residual signals. Mass spectra were obtained at the QB3/Chemistry Mass Spectrometry Facility, on a Finnigan LTQ FT high-resolution electrospray ionization (ESI) mass spectrometer. Yields indicate the amount of isolated material, and reactions were not optimized. Silica gel (230−400 mesh) was used for column chromatography purifications. Terephthalamide derivative **4** was prepared as described previously.[23]

*Bis(Cbz)tren (**1**).* Benzyl phenyl carbamate (Sigma-Aldrich, 20.5 mL, 103.8 mmol) was added dropwise to a stirring CH_2Cl_2 (50 mL, degassed) solution of tren (TCI, 7.0 mL, 46.8 mmol) in an ice bath. Following melting of the ice bath, the reaction was stirred at room temperature for 12 h. The clear, light yellow reaction mixture was reduced in vacuo to a yellow oil and purified by silica column chromatography (5−15% MeOH in DCM). The product fractions were rotary evaporated and further dried on the vacuum line for 8 h with light (50 °C) heating to a light yellow, translucent oil (72%). ^{1}H NMR (600 MHz, $CDCl_2$, δ): 2.45−2.65 (m, $NCH_2CH_2NH_2$ and NCH_2CH_2NHCbz, 8H), 3.24 (s, NCH_2CH_2NHCbz, 4H), 5.11 (s, Bn CH_2, 4H), 5.16 (br s, amine H, 1H), 6.57 (s, amide H, 2H), 7.33−7.36 (m, Ph H, 10H). ^{13}C NMR (151 MHz, $CDCl_2$, δ): 39.7, 40.0, 49.5, 54.5, 57.3, 66.6, 116.2, 119.2, 128.2, 128.7, 128.8, 129.8, 137.7, 157.3, 158.4. HRMS-ESI (m/z): $[M + H]^+$ calcd for $C_{22}H_{31}O_4N_4^+$ 415.2340, found 415.2333.

*Mono(Boc)-bis(Cbz)tren (**2**).* A solution of NaCl (4.789 g, 81.95 mmol) and $NaHCO_3$ (2.997 g, 35.67 mmol) in 60 mL water was added to a solution of **1** (10.2754 g, 24.05 mmol) in 50 mL of CH_2Cl_2. Di-*tert*-butyl dicarbonate (Sigma-Aldrich, 5.7373 g, 26.29 mmol) dissolved in 10 mL of CH_2Cl_2 was added to the biphasic mixture, resulting in immediate bubbling. The reaction was let stir at room temperature overnight, filtered, and extracted with CH_2Cl_2 (3 × 40 mL). The combined organic extracts were reduced to a viscous, clear, light yellow oil that was purified by silica column chromatography (0−10% MeOH in CH_2Cl_2). The product fractions were rotary evaporated to a clear, yellow, viscous oil (84%). ^{1}H NMR (500 MHz, $CDCl_2$, δ):

dx.doi.org/10.1021/ja503456r | J. Am. Chem. Soc. XXXX, XXX, XXX−XXX

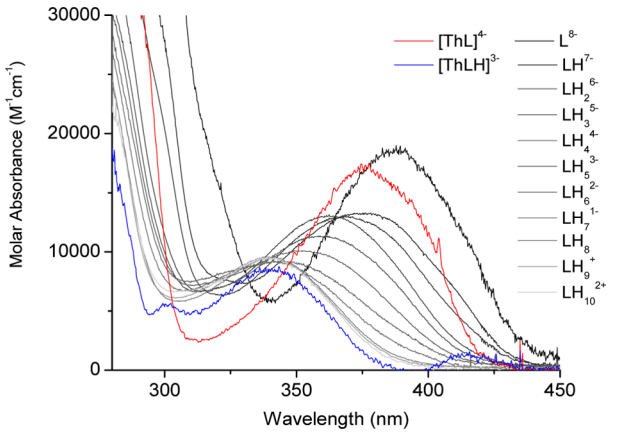

Figure 9. Molar extinction coefficients of species of **L** and Th**L**.

Table 4. log β_{mlh} and pTh Values for Various Ligands

	pH	L	DTPA	ETAM
log β_{110}		53.7(5)	28.78	45.54
log β_{111}; pK_a		58.9(6); 5.2(2)	30.94; 2.16	
pTh[a]	3.0	12.0	15.4	7.4
	7.4	39.1	25.6	19.4
	9.0	45.4	28.2 6	24.7

[a]pTh = $-\log[Th^{4+}]_{free}$; $[Th^{4+}]_{tot} = 10^{-6}$ M, $[L]_{tot} = 10^{-5}$ M.

1.36 (s, *t*-Bu, 9H), 2.51 (br t, NCH_2CH$_2$NHBoc, 2H), 2.54 (br t, NCH_2CH$_2$NHCbz, 4H), 3.10 (br t, NCH$_2$CH_2NHBoc, 2H), 3.19 (br t, NCH$_2$CH_2NHCbz, 4H), 5.05 (s, Bn H, 4H), 5.10 (br s, RN*H*Boc, 1H), 5.55 (br s, RN*H*Cbz, 2H), 7.28−7.32 (m, Ph H, 10H). ^{13}C NMR (151 MHz, CDCl$_2$, δ): 28.7, 39.2, 39.6, 54.6, 54.9, 66.9, 79.5, 128.4, 128.5, 128.9, 139.7, 157.2. HRMS-ESI (m/z): $[M + H]^+$ calcd for $C_{27}H_{39}O_6N_4^+$ 515.2864, found 515.2847.

*Mono(Boc)tren (**3**).* **2** (11.220 g, 20.20 mmol) was dissolved in 120 mL of MeOH in a glass vessel containing a magnetic stir bar. A 5 mL MeOH suspension of Pd/C (Sigma-Aldrich, 10 wt %, type E101 NE/W; 1.1318 g) was added to the solution and the glass vessel was placed in a Parr bomb. The bomb was purged three times with 750 psi of H_2 before being filled to 1250 psi of H_2. The reaction was stirred at room temperature for 24 h with a sustained pressure of 1000 psi. The reaction mixture was then filtered through a fine glass frit and rotary evaporated to a light yellow, viscous oil. The oil was coevaporated with MeOH on the vacuum line and dried for 24 h. NMR showed the presence of carbonate adduct in the product, which was dissolved in water and purified by elution through an ion-exchange column (Dowex 21K XLT resin). Evaporation afforded a clear, yellow oil (90%), which was stored at 4 °C as a CH_2Cl_2 solution containing 1 mol equiv of triethylamine. ^{1}H NMR (500 MHz, CDCl$_2$, δ): 1.38 (s, *t*-Bu, 9H), 2.44−2.49 (m, NCH_2CH$_2$NH$_2$ and NCH_2CH$_2$NHBoc, 6H), 2.66 (t, J = 6.0 Hz, 4H), 3.10 (br q, NCH$_2$CH_2NHBoc, 2H), 5.78 (br t, amine H, 1H). ^{13}C NMR (151 MHz, CDCl$_2$, δ): 28.7, 39.3, 40.0, 51.6, 57.8, 79.1, 156.8. HRMS-ESI (m/z): $[M + H]^+$ calcd for $C_{11}H_{27}O_2N_4^+$ 247.2129, found 247.2127.

*BnTAM(thiaz)(OMeEtN) (**7**).* A solution of 2-methoxyethanamine (Aldrich, 0.35 mL, 4.03 mmol) in 200 mL of $CHCl_3$ (with four drops of triethylamine) was added dropwise to a stirring solution of BnTAM(thiaz)$_2$ (**4**) (30.010 g, 51.7 mmol), in 1000 mL of CH_2Cl_2. The high-dilution slow addition was performed at room temperature over 16 h. The reaction mixture was then directly applied onto a gradient silica column (0−10% methanol in dichloromethane), and the desired product was eluted with 8% methanol. Rotary evaporation gave a yellow, foamy solid (91%) that became an oil upon storage at 4 °C. ^{1}H NMR (500 MHz, CD_2Cl_2): δ 3.03 (t, J = 9.0 Hz, 1H, methoxyethanamide CH$_2$), 3.24 (s, 3H, CH$_3$), 3.39−3.42 (m, 2H, thiaz CH$_2$), 3.47−3.51 (m, 2H, methoxyethanamide CH$_2$), 4.40 (t, J = 9.3 Hz, 2H, thiazolidine CH$_2$), 5.11 (s, 2H, Bn CH$_2$), 5.12 (s, 2H, Bn CH$_2$), 7.19 (d, J = 10.5 Hz, 1H, ArH), 7.35−7.43 (m, 10H, Ph), 7.84 (d, J = 10.5 Hz, 1H, ArH), 8.01 (br t, 1H, amide H). ^{13}C NMR (100 MHz, CD_2Cl_2): δ 28.8, 39.5, 55.7, 58.4, 70.8, 76.1, 76.7, 124.0, 126.4, 128.1, 128.4, 128.6, 128.6, 128.6, 128.9, 130.3, 133.6, 135.9, 137.1, 149.6, 150.2, 163.9, 166.7, 201.7. HRMS-ESI (m/z): $[M + H]^+$ calcd for $C_{28}H_{29}O_5N_2S_2^+$ 537.1512, found 537.1518.

*Mono(Boc)-bis(BnTAMthiaz)tren (**5**).* A solution of **3** (0.2792 g, 1.13 mmol) in 200 mL of $CHCl_3$ (with 3 drops of triethylamine) was added dropwise to a stirring solution of **4** (27.7 g, 47.7 mmol) in 500 mL of CH_2Cl_2 (with 5 drops triethylamine). The high-dilution slow addition was performed at room temperature over 18 h. The reaction mixture was reduced in volume by rotary evaporation and separated by silica column chromatography (2−5% MeOH in CH_2Cl_2). **5** was eluted with 4% methanol and was isolated as a yellow foamy solid after removal of the solvent (66%). ^{1}H NMR (500 MHz, CD_2Cl_2): δ 1.36 (s, 9H, CH$_3$), 2.39 (t, J = 6.5 Hz, 4H, tren CH$_2$), 2.46 (t, J = 6.0 Hz, 2H, tren CH$_2$), 2.99 (d, J = 6.0 Hz, 2H, tren CH$_2$), 3.03 (t, J = 7.3, 4H, tren CH$_2$), 3.23 (q, J = 6.2 Hz,4H, thiaz CH$_2$), 4.40 (t, J = 7.5 Hz, 4H, thiaz CH$_2$), 5.031 (br t, 1H, amide H), 5.10 (s, 4H, Bn CH$_2$), 5.12 (s, 4H, Bn CH$_2$), 7.17 (d, J = 8.0 Hz, 2H, ArH), 7.35−7.39 (m, 20H, Ph), 7.70 (d, J = 8.0 Hz, 2H, ArH), 7.76 (br t, 2H, amide H). ^{13}C NMR (100 Hz, CD_2Cl_2): δ 28.2, 28.9, 37.6, 55.7, 76.2, 76.8, 124.1, 126.2, 128.1, 128.4, 128.6, 128.7, 128.8, 128.9, 130.7, 133.4, 136.0, 137.1, 149.5, 150.1, 164.2, 166.7, 201.7. HRMS-ESI (m/z): $[M + H]^+$ calcd for $C_{61}H_{65}O_{10}N_6S_4^+$ 1169.3640, found 1169.3617.

*(TrenBoc)$_2$(BnTAM)$_2$ (**6**).* Two 450 mL $CHCl_3$ solutions, one of **5** (0.8503 g, 0.727 mmol) with 5 drops of triethylamine and one of **3** (0.19981 g, 0.811 mmol) with 15 drops of triethylamine, were combined by dropwise addition into a flask containing 1000 mL of CH_2Cl_2. The high-dilution addition took place over 72 h at room temperature. The reaction mixture became progressively less yellow, as the starting material **5** is yellow, but thiazolidine and TAM are colorless in solution. Since the reaction was still yellow once the addition was complete, diethylenetriamine (1 mL, 9 mmol) was added to the reaction mixture to facilitate separation from remaining **5**, as the primary amine renders its R_f on silica much lower. After 1.5 h, the reaction mixture had become colorless and was directly applied on a flash gradient silica column (0−3% MeOH in CH_2Cl_2). The product eluted with 3% methanol and was dried in vacuo to afford a white solid (87%). ^{1}H NMR (500 MHz, CD_2Cl_2): δ 1.33 (s, 18H, CH$_3$), 2.45 (br t, 4H, tren CH$_2$), 2.54 (t, J = 5.3 Hz, 8H, tren CH$_2$), 2.99 (br q, 4H, tren CH$_2$), 3.38 (q, J = 5.2 Hz, 8H, tren CH$_2$), 4.92 (br s, 2H, amide H), 5.03 (s, 8H, Bn CH$_2$), 7.10 (s, 4H, ArH), 7.36 (m, 20H, Ph), 7.67 (br s, 4H, amide H). ^{13}C NMR (100 MHz, CD_2Cl_2): δ 28.1, 37.1, 37.7, 52.6, 76.7, 78.7, 125.1, 128.4, 128.5, 128.6, 131.8, 136.6, 150.4, 155.8, 165.7. HRMS-ESI (m/z): $[M + H]^+$ calcd for $C_{66}H_{81}O_{12}N_{18}^+$ 1177.5968, found 1177.5962.

*Tren$_2$(BnTAM)$_2$[BnTAM(OMeEtN)] (**8**).* A solution of **6** (0.26435 g, 0.225 mmol) in 7 mL of CH_2Cl_2 was placed in an ice−water bath and stirred. Three milliliters of trifluoroacetic acid (TFA) was added dropwise over 5 min, and the reaction progress was monitored by TLC. The reaction mixture was stirred at 0 °C for 10 min and at room temperature for 20 min. The reaction mixture was dried in vacuo, affording a pink-orange oil that was redissolved in 2 mL of dichloromethane and subsequently dried in vacuo (this was performed twice). One milliliter of triethylamine and 1 mL of CH_2Cl_2 were added to the foamy oil at 0 °C, and the mixture was stirred at room temperature for 45 min before the addition of a solution of **7** (0.56 g, 1.05 mmol) in 8 mL of CH_2Cl_2. The reaction mixture was stirred at room temperature for 34 h. Separation of the product from triethylamine was achieved by extraction with 10 mL of water. The aqueous layer was acidified to pH 8 (from pH 10) with HCl and extracted with CH_2Cl_2 (3 × 5 mL). The combined organic layers were rotary evaporated and applied onto a gradient silica column (1−5% MeOH in CH_2Cl_2). The product was eluted with 5% methanol and further purified on a silica chromatron plate. The byproducts were eluted with 2.5% methanol in CH_2Cl_2, and a slow gradient to 6% was used to collect the desired product. Rotary evaporation resulted in a light yellow foamy solid (80%). ^{1}H NMR (500 MHz, CD_2Cl_2): δ 2.45 (t, J = 8.0 Hz, 4H, tren CH$_2$), 2.58 (t, J = 6.0 Hz, 8H, tren CH$_2$), 3.21

dx.doi.org/10.1021/ja503456r | J. Am. Chem. Soc. XXXX, XXX, XXX−XXX

(s, 6H, CH_3), 3.23−3.28 (m, 4H, methoxyethanamide CH_2), 3.37−3.41 (m, 12H, methoxyethanamide CH_2, tren CH_2), 3.49 (q, J = 6.7 Hz, tren CH_2), 4.89 (s, 8H, Bn CH_2), 5.06 (s, 4H, Bn CH_2), 5.07 (s, 4H, Bn CH_2), 6.90 (s, 4H, ArH), 7.31−7.42 (m, 40H, Ph), 7.43 (d, J = 10.5 Hz, 2H, ArH), 7.49 (d, J = 10.5 Hz, 2H, ArH), 7.62 (t, J = 6.5 Hz, 2H, amide H), 7.69 (t, J = 6.5 Hz, 4H, amide H), 8.07 (t, J = 5.5 Hz, 2H, amide H). ^{13}C NMR (100 MHz, CD_2Cl_2): δ 36.7, 37.0, 39.6, 51.8, 52.4, 58.3, 70.6, 76.3, 76.8, 76.9, 124.7, 125.4, 125.8, 128.3, 128.3, 128.5, 128.5, 128.5, 128.6, 130.2, 132.0, 136.1, 136.3, 136.7, 150.3, 150.5, 150.5, 164.3, 164.7, 164.7. HRMS-ESI (m/z): $[M + Na]^+$ calcd for $C_{106}H_{110}O_{18}N_{10}Na^+$ 1833.7892, found 1833.7866.

LH_8·3HCl. A 5 mL portion of 12.1 N HCl was added to a solution of **8** (0.32466 g, 0.179 mmol) dissolved in 5 mL of glacial acetic acid. The solution was stirred at room temperature for 64 h and dried in vacuo. The resulting light yellow cake was suspended in 10 mL of MeOH and dried 3 times to give a light yellow solid. Further drying of this solid under vacuum overnight yielded a light gray solid (89%). ^{1}H NMR (500 MHz, D_2O + NaOD): δ 2.883 (t, J = 7.3 Hz, 4H, tren CH_2), 2.93 (t, J = 6.0 Hz, 8H, tren CH_2), 3.34 (s, 6H, CH_3), 3.41 (t, 6.3 Hz, 8H), 3.49−3.53 (m, 8H, tren CH_2, methoxyethanamide CH_2), 3.60 (t, J = 5.5 Hz, 4H, methoxyethanamide CH_2), 6.54 (s, 4H, ArH), 6.87 (s, 2H, ArH), 6.87 (s, 2H, ArH). ^{13}C NMR (125 Hz, DMSO-d_6): δ 34.3, 34.4, 39.5, 49.0, 50.4, 51.6, 51.9, 58.4, 70.5, 116.6, 116.7, 116.9, 117.0, 117.3, 118.4, 119.6, 149.5, 150.5, 150.6, 150.9, 169.0, 169.1, 170.8. HRMS-ESI (m/z): $[M + Na]^+$ calcd for $C_{50}H_{62}O_{18}N_{10}Na^+$ 1113.4136, found 1113.4126; $[M - H]^-$ calcd for $C_{50}H_{61}O_{18}N_{10}^-$ 1089.4171, found 1089.4170. Anal. Calcd (found) for $C_{50}H_{62}O_{18}N_{10}$·3HCl: C, 50.03 (50.38); H, 5.46 (5.58); N, 11.67 (11.51). 11.51. Anal. Calcd (found) for $C_{50}H_{62}O_{18}N_{10}$·3HCl (Columbia Analytical Services): C, 50.03 (50.01); Cl, 8.9 (7.0); H, 5.46 (5.64); N, 11.67 (11.30).

*[Th***L***]4K.* **L**H_8·3HCl (13.65 mg, 0.0114 mmol) was suspended in 7 mL of methanol at 45 °C. A solution of $Th(NO_3)_4$·$4H_2O$ (Alfa, 6.12 mg, 0.0111 mmol) in 1 mL of MeOH was added dropwise to the ligand solution while stirring, causing an immediate color change to yellow. A stoichiometric amount of 1 M KOH in methanol (0.09 mL, 0.0910 mmol) was added to the ligand suspension dropwise, to a pH of 8, solubilizing the reaction mixture. (The thorium solution can be added after the base.) The reaction mixture was refluxed under nitrogen flow for 3 h. Once cooled to room temperature, the product was precipitated by addition of diethyl ether and concentration of the reaction mixture. The tan precipitate was filtered and dried overnight under vacuum, resulting in a light brown solid (15.11 mg, 93%). ^{1}H NMR (500 MHz, D_2O + NaOD + DMSO-d_6): 2.264 (br t, 2H, tren CH_2), 2.365 (br t, 4H, tren CH_2), 2.647 (br t, 4H, tren CH_2), 3.069 (s, 6H, CH_3), 3.133−3.259 (m, 14H, tren CH_2, methoxyethanamide CH_2), 3.510 (d, J = 10 Hz), 4H, methoxyethanamide CH_2), 3.743 (d, J = 11.5 Hz, tren CH_2), 6.662−6.681 (d, 2H, ArH; s, 4H, ArH), 6.785 (d, J = 8.5 Hz, ArH). ^{13}C NMR (125 Hz, DMSO-d_6): δ 36.2, 38.2, 38.8, 40.3, 56.1, 58.3, 58.4, 58.5, 70.8, 72.2, 109.6, 109.8, 114.5, 114.6, 114.7, 168.3, 168.5, 168.9, 169.0, 171.0, 171.2, 171.4. HRMS-ESI (m/z): $[M + H]^{3-}$ calcd for $C_{50}H_{54}O_{18}N_{10}Th^{3-}$ 438.1338, found 438.1355.

X-ray Crystallography. Single crystals of **L**H_8 suitable for XRD were grown by the vapor diffusion of acetonitrile into an aqueous solution of the protonated ligand. Single crystals of Th**L**K_4 were grown by the vapor diffusion of 1:1 diethyl ether:tetrahydrofuran into a solution of the complex in 1:20 dimethylformamide:methanol. Selected crystals were mounted in Paratone N oil at the end of a captan loop and frozen in place under a low-temperature nitrogen stream. The data were collected on Bruker MicroSTAR-H X8 APEX-II CCD with Cu Kα radiation (**L**H_8) or SMART APEX-I CCD with Mo Kα radiation (Th**L**K_4) X-ray diffractometers. Intensity data were extracted from the frames with the program APEX2. The data were corrected for Lorentz and polarization effects, and an empirical absorption correction was applied using the SADABS program.[24] The structures were solved by direct methods and refined using full-matrix least-squares refinements based on F^2 in SHELXL-97.[25] Crystallographic analyses were performed using the WinGX system of programs.[26] All non-hydrogen atoms were refined anisotropically, while hydrogen atoms were assigned to idealized positions (with the exception of the hydrogens in **L**H_8 bound to heteroatoms and aromatic rings). The free ligand crystallized with two chlorine atoms (balancing the charge on the protonated tertiary amines) and four water molecules per ligand molecule. The thorium complex crystallized with four potassium atoms, as well as two dimethylformamide, one tetrahydrofuran, and two methanol molecules per asymmetric unit. Disordered solvent molecules in this crystal structure (all but one methanol) were modeled with occupancies of less than 1. One of the methoxyethyl substituents (atoms C37, O18, C38 and the attached hydrogens) on the pendant terephthalamide units showed some disorder, which could be satisfactorily modeled over two positions. The structure diagrams in Figure 2 were created using ORTEP-32.[27]

Computational Studies. DFT calculations were performed at the UC Berkeley Molecular Graphics and Computation Facility with Gaussian 09 software and the GaussView graphical user interface.[28] The geometries and energies of the complexes were optimized at the B3LYP level with the 6-31G basis set for all atoms except the thorium atoms, for which the Stuttgart/Dresden ECP60MWB_SEG basis set was used to model a 60-electron small core pseudopotential, incorporating quasi-relativistic effects.[10]

Kinetic Studies. *Indirect Kinetics.* Arsenazo III (Sigma-Aldrich) was twice purified by HPLC prior to use. The dye (100 mg) was dissolved in Millipore water, filtered through a 0.22 uM nylon syringe filter, and separated on a preparatory Varian Dynamax 250 × 41.1 mm C_{18} column. A solvent gradient of 0−18% acetonitrile/H_2O (0.1% TFA) was used to collect three fractions with intense UV absorbances. The fraction with the most intense absorbance (t_R 15−16 min) was collected as the main product, without the front or back tailing material. This fraction was rotary evaporated, and the dark purple-green solid was resuspended in methanol before drying under vacuum overnight. HRMS-ESI (m/z): $[M - 2H]^{2-}$ calcd for $C_{22}H_{16}As_2O_{14}N_4S_2^{2-}$ 386.9274, found 386.9279. Anal. Calcd (found) for $C_{22}H_{18}As_2O_{14}N_4S_2$·$2H_2O$: C, 32.53 (32.34); H, 2.73 (2.73); N, 6.90 (6.71).

UV−vis spectra were acquired on a Hewlett-Packard 8453 diode array spectrometer at 25 °C. The temperature was controlled by a recirculating water bath connected to the jacketed cell holder. Samples were measured in small volume (50 μL) quartz cuvettes with 1 cm path lengths. Solutions were buffered with 100 mM HEPES at pH 7.4 (at 25 °C, with 0.1 M KCl). Complexation of the thorium and dye was performed by combining aqueous stock solutions of standardized Th^{4+} in nitric acid (pH 1.4, 1 mM, diluted from a 10 mM solution, the standardization is described in the next section) and an excess of purified dye (1 mM). The solution was let sit on the bench at room temperature for 30 min, diluted in buffer, and let sit at room temperature for 1 h. The absorbance was monitored starting from the addition of ligand, as a solution of DMSO ligand stock solution (5 mM) and buffer (equilibrated for 15 min beforehand). DOTA was purchased from Sigma-Aldrich. The A vs t plots were fit with a first-order decay equation in Origin 6.1 at wavelengths corresponding to the appearance of free dye (550, 560 nm) and the disappearance of thorium−dye complex (614, 669, 700 nm).

Stopped-Flow Kinetics. The stopped-flow kinetic experiments were performed using a stopped-flow apparatus equipped with an OLis rapid-scanning monochromator 1000 and a 75 W Xe lamp. Upon electronic activation, the apparatus (powered by Ar flow) mixes 100 μL of each solution in the two syringes into a mixing chamber. This mixture is injected into a separate chamber, where the flow is stopped and UV spectra are taken. One syringe contained 10 μM Th^{4+} in 79 mM HNO_3 (pH 1.4), while the other held a solution of 50−300 μM ligand, in 200 mM HEPES (pH 8.3) and 10% DMSO. The 1:1 mixture of these solutions was 5 μM Th, 25−150 μM ligand, 100 mM HEPES (pH 7.4). UV spectra in the 305−454 nm range were collected for 1.5−10 s, depending on the concentrations of the starting materials, at rates of 31−1000 scans/s. The data were analyzed using the program SpecFit to simultaneously use the absorbance at all of the wavelengths to obtain a second-order rate constant.

Solution Thermodynamics. All spectrophotometric titrations were carried out with constant stirring and a blanket of Ar flow in a jacketed cell connected to a recirculating water bath to maintain the temperature at 25 °C. The ionic strength of all solutions was

maintained at 0.1 M with 0.1 M KCl in titrand solutions and 0.1 M acid and base titrants. A standardized stock solution of 0.0010(1) M Th^{4+} was prepared by dissolving $Th(NO_3)_4{\cdot}4H_2O$ (Alfa Products) in Millipore water with concentrated HNO_3 (79 mM, pH 1.4). This solution was complexometrically titrated with Na_2H_2EDTA (volumetric standard, Sigma-Aldrich) to the yellow end point, using pyrocatechol violet as the indicator.[29] **L** was added as a 50 mM DMSO solution, prepared by dissolution of the solid ligand, weighed on an analytical balance accurate to 0.01 mg. The HCl and KOH solutions were prepared by dilution of Dilut-It (J.T. Baker, ampules) concentrated solutions with degassed Millipore water. The 0.1 M HCl solution was standardized by the potentiometric or colorimetric (using bromocresol green as indicator) titration of tris-(hydroxymethyl)aminomethane, and the 0.1 M KOH solution was standardized by potentiometric titration of potassium hydrogen phthalate or the standardized HCl solution. The KOH solution was stored under a blanket of Ar flow and standardized before every titration. The glass electrode (Metrohm Microtrode) used for the pH measurements was calibrated by the titration of 1.000 mL of standardized 0.1 M HCl in 25.0 mL of 0.1 M KCl with standardized 0.1 M KOH to pH 11.6. The titration was analyzed using the program GLEE[30] to refine for the E° and slope. This calibration was also performed prior to each titration. The automated titration system was controlled by a Metrohm Titrando 907 and the program Tiamo light. Two-milliliter Dosino 800 burets dosed the titrant into the titration vessel (5−90 mL). UV−vis spectra were acquired with an Ocean Optics USB4000-UV−vis spectrometer equipped with a dip probe (set to a 10 mm path length) and a DH-2000 light source (deuterium and tungsten lamps), using the program Spectra Suite. Titrations were performed at least in triplicate.

Ligand Titration. Ten-milliliter solutions of 50 μM ligand and 20 equiv (1 mM) each of MES, HEPES, and CHES were titrated forward and backward between pH 1.8 and 12.7 with standardized 0.1 M KOH and 0.1 M HCl. Data points (pH readings and UV−vis spectra) were collected following 0.040−1.000 mL titrant additions, with an equilibration time of 180 s. The 1 mL titrant additions were performed above pH 11 due to the buffering capacity of water at high pH and to minimize the exposure of the electrode to basic solution; 0.1 M HCl was added to the solution prior to the forward titration to start at a pH below 2. All absorbance measurements used in the refinement were no more than 1.0 absorbance units. Spectra at 250−450 nm (at intervals of approximately 0.1 nm) were analyzed (simultaneously) with the program Hypspec.[31]

Th^{4+} Competition Titration. Ten-milliliter solutions of 50 μM **L**, 50 μM Th^{4+}, and 500 μM DTPA (Pharm-Eco) were titrated forward and backward with between pH 1.8 and 10.0 with 0.1 M KOH and 0.1 M HCl. The Th^{4+} was added to a solution of DTPA at pH 7.4, and this solution was allowed to equilibrate for at least 24 h prior to the addition of **L**. The data points (pH readings and UV−vis spectra) were collected following 0.040−0.100 mL of titrant, with an equilibration time of 10 min following KOH additions (forward titrations) or 20 min following HCl additions (backward titrations); 0.1 M HCl was added to the solution prior to the forward titration to start at a pH below 2. All absorbance measurements used in the refinement were no more than 1.1 absorbance units. Spectra of 250−450 nm (at intervals of approximately 0.1 nm) were analyzed (simultaneously) with the program Hypspec. The following values for the log β for the formation of Th hydroxides were included in the refinement: $[ThOH]^{3+}$, −2.5; $[Th(OH)_2]^{2+}$, −6.2; $Th(OH)_4$, −17.4; $[Th_2(OH)_2]^{6+}$, −5.9; $[Th_2(OH)_3]^{5+}$, −6.8; $[Th_4(OH)_8]^{8+}$, −20.4; $[Th_4(OH)_{12}]^{4+}$, −26.6; $[Th_6(OH)_{14}]^{10+}$, −36.8; $[Th_6(OH)_{15}]^{9+}$, −36.8.[16] The following protonation and stability constants for DTPA and the Th−DTPA complex were also included: logβ_{011}, 10.4; log β_{012}, 18.95; log β_{013}, 23.23; log β_{014}, 25.93; log β_{015}, 27.93; log β_{016}, 29.53; log β_{017}, 30.23; log β_{110}, 28.78; log β_{111}, 30.94; log β_{11-1}, −8.88.[21,32] Spectra and protonation constants of the free ligand, refined from the ligand titrations, were set constant in the refinement.

■ ASSOCIATED CONTENT

Ⓢ Supporting Information

CIF files for LH_8 and $ThLK_4$. This material is available free of charge via the Internet at http://pubs.acs.org.

■ AUTHOR INFORMATION

Corresponding Author

raymond@socrates.berkeley.edu

Notes

The authors declare the following competing financial interest(s): Kenneth N. Raymond has a financial interest in Lumiphore Inc., which has licensed University of California technology in this general field.

■ ACKNOWLEDGMENTS

This research is supported by the Director, Office of Science, Office of Basic Energy Sciences, and the Division of Chemical Sciences, Geosciences, and Biosciences of the U.S. Department of Energy at LBNL under Contract No. DE-AC02-05CH11231. The authors would like to thank Dr. Manuel Sturzbecher-Hoehne and Dr. Peter Gans for their help with titrations, Dr. Antonio DiPasquale for his help with the XRD data, and Dr. Casey J. Brown for helpful discussions. The computational work was made possible by NSF grant CHE-0840505, which funds the UC Berkeley Molecular Graphics Facility.

■ REFERENCES

(1) (a) Lawrence, J. H.; Tobias, C. A.; Born, J. L. *Trans. Am. Clin. Climatol. Assoc.* **1961**, *73*, 176−185. (b) Lawrence, J. H.; Tobias, C. A.; Born, J. L.; Gottschalk, A.; Linfoot, J. A.; Kling, R. P. *J. Am. Med. Assoc.* **1963**, *186*, 236−245. (c) Lawrence, J. H.; Tobias, C. A.; Born, J. L.; Linfoot, J. A.; Kling, R. P.; Gottschalk, A. *Trans. Am. Clin. Climatol. Assoc.* **1964**, *75*, 111−116. (d) Kim, Y.-S.; Brechbiel, M. W. *Tumor Biol.* **2012**, *33*, 573−590.

(2) (a) Barendsen, G. W.; Beusker, T. L. J.; Vergroesen, A. J.; Budke, L. *Radiat. Res.* **1960**, *13*, 841−849. (b) Ritter, M. A.; Cleaver, J. E.; Tobias, C. A. *Nature* **1977**, *266*, 653−655.

(3) Kluetz, P. G.; Pierce, W.; Maher, V. E.; Zhang, H.; Tang, S.; Song, P.; Liu, Q.; Haber, M. T.; Leutzinger, E. E.; Al-Hakim, A.; Chen, W.; Palmby, T.; Alebachew, E.; Sridhara, R.; Ibrahim, A.; Justice, R.; Pazdur, R. *Clin. Cancer Res.* **2014**, *20*, 9−14.

(4) (a) Dahle, J.; Krogh, C.; Melhus, K. B.; Borrebaek, J.; Larsen, R. H.; Kvinnsland, Y. *Int. J. Radiat. Oncol. Biol. Phys.* **2009**, *75*, 886−895. (b) Miederer, M.; Scheinberg, D. A.; McDevitt, M. *Adv. Drug Delivery Rev.* **2008**, *60*, 1371−1382. (c) Boswell, C. A.; Brechbiel, M. W. *Nucl. Med. Biol.* **2007**, *34* (7), 757−778. (d) Zalutsky, M. R.; Pozzi, O. R. *Q. J. Med. Mol. Imaging* **2004**, *48*, 289−296.

(5) Larsen, R.; Bruland, Oeyvind, B. Thorium-227 for Use in Radiotherapy of Soft Tissue Disease. WO2004091668A1, October 28, 2004.

(6) (a) Harrison, A.; Walker, C. A.; Parker, D.; Jankowski, K. J.; Cox, J. P. L.; Craig, A. S.; Sansom, J. M.; Beeley, N. R. A.; Boyce, R. A.; Chaplin, L.; Eaton, M. A. W.; Farnsworth, A. P. H.; Millar, K.; Millican, A. T.; Randall, A. M.; Rhind, S. K.; Secher, D. S.; Turner, A. *Nucl. Med. Biol.* **1991**, *18* (5), 469−476. (b) Ruegg, C. L.; Anderson-Berg, W. T.; Brechbiel, M. W.; Mirzadeh, S.; Gansow, O. A.; Strand, M. *Cancer Res.* **1990**, *50* (14), 4221−4226. (c) Kodama, M.; Koike, T.; Mahatma, A. B.; Kimura, E. *Inorg. Chem.* **1991**, *30*, 1270−1273.

(7) (a) Gorden, A. E. V.; Raymond, K. N. *Chem. Rev.* **2003**, *103*, 4207−4282. (b) Gramer, C. J.; Raymond, K. N. *Inorg. Chem.* **2004**, *43*, 6397−6402. (c) Durbin, P. W. *Health Phys.* **2008**, *95* (5), 465−492. (d) Abergel, R. A.; Raymond, K. N. *Hemoglobin* **2011**, *35*, 276−290.

(8) Benito, J. M.; Gomez-Garcia, M.; Mellet, C. O.; Baussane, I.; Defaye, J.; Garcia Fernandez, J. M. *J. Am. Chem. Soc.* **2004**, *126*, 10355−10363.
(9) A recent application of the high-dilution technique is featured here: Xu, J.; Corneillie, T. M.; Moore, E. G.; Law, G.-L.; Butlin, N. G.; Raymond, K. N. *J. Am. Chem. Soc.* **2011**, *133* (49), 19900−19910.
(10) (a) Becke, A. D. *J. Chem. Phys.* **1993**, *98*, 5648−5652. (b) Miehlich, B.; Savin, A.; Stoll, H.; Preuss, H. *Chem. Phys. Lett.* **1989**, *157*, 200−206. (c) Lee, C.; Yang, W.; Parr, G. *Phys. Rev. B* **1988**, *37*, 785−789. (d) Hehre, W. J.; Ditchfield, R.; Pople, J. A. *J. Chem. Phys.* **1972**, *56*, 2257−2261. (e) http://www.theochem.uni-stuttgart.de/pseudopotentials/clickpse.en.html. (f) Haeusermann, U.; Dolg, M.; Stoll, H.; Preuss, H. *Mol. Phys.* **1993**, *78*, 1211−1224. (g) Leininger, T.; Nicklass, A.; Stoll, H.; Dolg, M.; Schwerdtfeger, P. *J. Chem. Phys.* **1996**, *105*, 1052−1059. (h) Kuechle, W.; Dolg, M.; Stoll, H.; Preuss, H. *J. Chem. Phys.* **1994**, *100*, 7535−7542. (i) Cao, X.; Dolg, M.; Stoll, H. *J. Chem. Phys.* **2003**, *118*, 487−496. (j) Cao, X.; Dolg, M. *J. Mol. Struct. (THEOCHEM)* **2004**, *673*, 203−209.
(11) An algorithm for calculating the dihedral angles in a coordination polyhedron (only taking into account the metal and donor atoms) and minimizing their variance from those of idealized polyhedra was written some years ago (Xu, J.; Radkov, E.; Ziegler, M.; Raymond, K. N. *Inorg. Chem.* **2000**, *39*, 4156−4164) and recently updated (Tatum, D.; Raymond, K.N. Automated δ dihedral angle shape analysis for coordination numbers four through nine. Manuscript in preparation.). The values stated here were calculated using the updated algorithm..
(12) The *m* edges of the trigonal dodecahedron are those lying on the mirror planes: Hoard, J. L.; Silverton, J. V. *Inorg. Chem.* **1963**, *2*, 235−250 . An ideal trigonal dodecahedron for the Th**L** complex was generated by rotation of the binding unit with the smallest deviation about the pseudo-S_4 axis of the inner coordination environment. The angles of deviation of the TAMs from ideal *m* edges were then calculated from the superposition of the crystal structure coordinates onto this ideal dodecahedron..
(13) Busch, D. H.; Farmery, K.; Goedken, V.; Katovic, V.; Melnyk, A. C.; Sperati, C. R.; Tokel, N. *Adv. Chem. Ser.* **1971**, *100*, 44.
(14) (a) Wang, X. W.; Jin, T.; Comblin, V.; Lopez-Mut, A.; Merciny, E.; Desreux, J. F. *Inorg. Chem.* **1992**, *31*, 1095−1099. (b) Choi, K.; Hong, C. P. *Bull. Korean Chem. Soc.* **1994**, *15* (4), 293−297.
(15) (a) Leon-Rodriguez, L. M.; Kovacs, Z. *Bioconjugate Chem.* **2008**, *19* (2), 391−402. (b) Viola-Villegas, N.; Doyle, R. P. *Coord. Chem. Rev.* **2009**, *253* (13−14), 1906−1925.
(16) Rand, M.; Fuger, J.; Grenthe, I.; Neck, V.; Rai, D. In *Chemical Thermodynamics of Thorium*; Monpean, F. J., Perrone, J., Illemassene, M., Eds.; OECD Nuclear Energy Agency (NEA) "Chemical Thermodynamics" series; OECD Publishing: Paris, France, 2007; Vol. *11*, p 170.
(17) Binstead, R. A.; Zuberbuhler, A. D.; Jung, B. *Specfit, version 3.0.30*, 1993−2002.
(18) Basargin, N. N.; Ivanov, V. M.; Kuznetsov, V. V.l; Mikhailova. *J. Anal. Chem.* **2000**, *55*, 204−210.
(19) (a) Stradling, G. N.; Gray, S. A.; Pearce, M. J.; Wilson, I.; Moody, J. C.; Burgada, R.; Durbin, P. W.; Raymond, K. N. *Human Exp. Toxicol.* **1995**, *14*, 165−169. (b) Stradling, G. N.; Hodgson, S. A.; Pearce, M. J. *Radiat. Prot. Dosim.* **1998**, *79*, 445.
(20) Garrett, T. M.; Miller, P. W.; Raymond, K. N. *Inorg. Chem.* **1989**, *28*, 128−133.
(21) Brown, M. A.; Paulenova, A.; Gelis, A. V. *Inorg. Chem.* **2012**, *51* (14), 7741−7748.
(22) Harris, W. R.; Carrano, C. J.; Cooper, S. R.; Sofen, S. R.; Avdeef, A.; McArdle, J. V.; Raymond, K. N. *J. Am. Chem. Soc.* **1979**, *101*, 6097−6104.
(23) (a) Doble, D. M. J.; Melchior, M.; O'Sullivan, B.; Siering, C.; Xu, J.; Pierre, V. C.; Raymond, K. N. *Inorg. Chem.* **2003**, *42*, 4930−4937. An alternative synthesis also yields desired product: (b) Nagao, Y.; Miyasaka, T.; Hagiwara, Y.; Fujita, E. J. *Chem. Soc. Perkin Trans. 1* **1984**, 183−187.
(24) SADABS: Bruker Nonius Area Detector Scaling and Absorption V. 2.05; Bruker Analytical X-ray Systems, Inc.: Madison, WI, 2003.
(25) Sheldrick, G. M. *Acta Crystallogr.* **2008**, *A64*, 112−122.
(26) Farrugia, L. J. *J. Appl. Crystallogr.* **1999**, *32*, 837.
(27) ORTEP-3 for Windows: Farrugia, L. J. *J. Appl. Crystallogr.* **1997**, *30*, 565.
(28) Frisch, M. J.; Trucks, G. W.; Schlegel, H. B.; Scuseria, G. E.; Robb, M. A.; Cheeseman, J. R.; Scalmani, G.; Barone,V.; Mennucci, B.; Petersson, G. A., Nakatsuji, H.; Caricato, M.; Li, X.; Hratchian, H. P.; Izmaylov, A. F.; Bloino, J.; Zheng, G.; Sonnenberg, J. L.; Hada, M.; Ehara, M.; Toyota,K.; Fukuda, R.; Hasegawa, J.; Ishida, M.; Nakajima, T.; Honda, Y.; Kitao, O.; Nakai, H.; Vreven, T.; Montgomery, J. A., Jr.; Peralta, J. E.; Ogliaro, F.; Bearpark, M.; Heyd, J. J.; Brothers, E.; Kudin, K. N.; Staroverov, V. N.; Keith,T.; Kobayashi, R.; Normand, J.; Raghavachari, K.; Rendell, A.; Burant, J. C.; Iyengar, S. S.; Tomasi, J.; Cossi, M.; Rega, N.; Millam, J. M.; Klene,M.; Knox, J. E.; Cross, J. B.; Bakken, V.; Adamo, C.; Jaramillo, J.; Gomperts, R.; Stratmann, R. E.; Yazyev,O.; Austin, A. J.; Cammi, R.; Pomelli,C.; Ochterski, J. W.; Martin, R. L.; Morokuma, K.; Zakrzewski, V. G.; Voth, G. A.; Salvador, P.; Dannenberg, J. J.; Dapprich, S.; Daniels, A. D.; Farkas, O.; Foresman, J. B.; Ortiz, J. V.; Cioslowski, J.; Fox, D. J. *Gaussian 09, Revision B.01*; Gaussian, Inc.: Wallingford, CT, 2010.
(29) Schwarzenbach, G. *Complexometric Titrations*; Interscience Publishers: New York, 1957; p 75−76.
(30) Gans, P.; O'Sullivan, B. *Talanta* **2000**, *51*, 33−37.
(31) (a) Gans, P.; Sabatini, A.; Vacca, A. *Talanta* **1996**, *43*, 1739−1753. (b) Gans, P.; Sabatini, A.; Vacca, A. *Ann. Chim.* **1999**, *89*, 45−49.
(32) *NIST Standard Reference Database 46: NIST Critically Selected Stability Constants of Metal Complexes Database, Version 8.0*, U.S. Department of Commerce, 2004.